EXPERIMENTAL AND ANALYTICAL INVESTIGATION OF THE VARIATION OF SPRAY CHARACTERISTICS ALONG A RADIAL DISTANCE DOWNSTREAM OF A PRESSURE-SWIRL ATOMIZER

J.S. Chin, W.M. Li, and X.F. Wang
Beijing Institute of Aeronautics and Astronautics
Beijing, People's Republic of China

The variation of spray characteristics along a radial distance downstream of a pressure-swirl atomizer was measured by laser light-scattering technology. An analytical model was developed to predict the variation of spray characteristics along the radial distance. A comparison of the predicted and experimental data showed excellent agreement. Therefore, the spray model proposed, although relatively simple, is correct and can be used, with some expansion and modification of the prepared model, to predict more complicated spray systems.

INTRODUCTION

The characteristics of the spray formed by an atomizer in a liquid-fueled combustion device are extremely important to the performance, stability, and pollutant formation of the combustor. The spray characteristics should be measured accurately, and a model should be developed to predict the variation of spray characteristics, droplet trajectory, spray dispersion, and evaporation history. It is also important to understand the influence of various factors on the measurement of spray characteristics. A comparison between predicted and measured spray characteristics provides useful insight into spray combustion. Such research has a significant effect on engineering applications and on the fundamental understanding of spray combustion.

The authors analyzed the variation of spray characteristics along the axial distance downstream of a pressure-swirl atomizer. The effect of spray evaporation on the variation of spray characteristics is discussed in reference 1 and was presented by J.S. Chin and J.Y. Zhu at this symposium. (Paper, entitled The Interdependence of Spray Characteristics and Evaporation History of Fuel Sprays in High Temperature Airflows, was unavailable for printing at the time of publication.) The influence of downstream distance on the spray characteristics of pressure-swirl atomizers is caused by the effects of spray dispersion and drop acceleration or deceleration. This condition is analyzed in reference 2. These analyses have been partially substantiated by some experimental data. Until now there have been few experimental data of the variation of spray characteristics along the radial distance downstream of the pressure-swirl atomizer. Lee Dodge published his measurement results as shown in figure 1 (ref. 3). He shows that both the Sauter mean diameter SMD and drop-size distribution parameter N increase with radial distance. There is no analysis on this aspect available at the present time.

We are interested in comparing the experimental and predicted values of the variation of spray characteristics along the radial distance. Therefore, we carefully measured this variation in a well-defined experimental condition, developed an analytical model to predict the variation, and then compared the

experimental and predicted data. These comparisons promote our understanding of spray dispersion and the factors influencing drop-size measurement. After we have predicted the simple spray system, we will be able to expand and modify the proposed spray model to extend its capability to more complicated spray systems.

Cao and Chin proposed a flat-fan spray model for the fuel distribution downstream of a plain orifice injector under cross airflow (ref. 4). The model was validated by fuel distribution measured by gas analysis and drop size. It is obvious that, for the validation of a given spray model, the spray characteristics measurement is reliably accurate and much simpler than the fuel distribution measurement. It is this author's intention to validate a spray model by measuring the spray characteristics along the radial distance. The same spray model has also been validated by measuring the spray characteristics along different θ angles (as shown in fig. 5).

TEST APPARATUS, ATOMIZER, AND PARTICLE SIZER

The test section was a rectangular chamber with transparent windows for optical drop-size measurement. The test apparatus included an air system and a fuel system, as shown in figure 2.

The atomizer tested (fig. 3) was a pressure-swirl atomizer taken from an existing aircraft gas-turbine engine. The atomizer had a pilot-fuel flow and a main-fuel flow. In this test we used the pilot-fuel passage. Because the flow rate is relatively lower with pilot-fuel flow, the obscuration was in the right range.

A Malvern drop-size analyzer model 2200 was used. The principle of the particle sizer is shown in figure 4. The instrument was set on the Rosin-Rammler distribution mode. The direct results from the instrument are the characteristic diameter $\bar{D}$ and the drop-size distribution parameter N in the R-R distribution which is expressed by

$$Q = 1 - \exp\left[-\left(\frac{D}{\bar{D}}\right)^N\right] \tag{1}$$

where Q is the fraction of the total volume contained in drops that have a diameter less than D.

The Sauter mean diameter SMD can be obtained from

$$SMD = \bar{D}\left[\Gamma\left(1 - \frac{1}{N}\right)\right]^{-1} \tag{2}$$

where Γ is the gamma function.

EXPERIMENTAL RESULTS

During drop-size measurement tests, the laser light beam was first adjusted so that it was in the same horizontal plane as the central line of the atomizer and that it was perpendicular to this central line. At this

position (defined as the $y = 0$ position), the spray characteristics were measured. Then the Malvern particle sizer was put on some size blocks of known dimension. This changed the height of the laser beam so that the radial distance where the particle sizer measured the drop size was changed. The summation of the size block was defined as the radial distance y. The dimensions of the blocks chosen were 2.5, 3.0, and 10 mm. Thus, the following radial distance y could be obtained by different combinations of the size blocks: $y = 0$, 5.5, 10.0, 15.5, 20.0, 25.5, and 30.0 mm. The experimental results are shown in figures 6 to 13. From these figures it is clear that the Sauter mean diameter and drop-size distribution parameter increase with radial distance until the edge of the spray has been reached. The experimental results obtained by the present authors are quantitatively in good agreement with Lee Dodge's results. The obvious explanation of the measured results shown in figures 6 to 13 is that with larger radial distances the possibility of the laser light beam meeting the large drops is greater than it is with smaller radial distances. This shows that when we measure the drop size it is necessary to take a sample that is representative of the spray formed; however, it is impossible to define the sample which would fully represent the spray. The most reasonable sample can be obtained by measuring the spray at the $y = 0$ position.

Comparing figure 6 with 8 and 7 with 9 shows that, at a higher airflow velocity, the change of spray characteristics along the radial distance is weaker. A comparison of figures 8, 10, and 12 and of 9, 11, and 13 shows that, with a lower pressure drop across the nozzle, the change of the spray characteristics along the radial distance is weaker. These results tell us that when the spray is expanded less radially the change of spray characteristics is also flatter. The reverse is also true.

The experimental data obtained in this way were used to check the proposed spray model.

PHYSICAL MODEL

The spray formed by a pressure-swirl atomizer is shown in figure 5. The physical model was proposed with the following assumptions:

(1) The atomization process is completed as soon as the fuel leaves the atomizer nozzle; that is, droplets of different sizes start their movement at the nozzle exit. Droplets of different sizes have the same initial velocity. Because it is suitable to use a cylindrical coordinate system to describe droplet motion, the tangential velocity and the radial velocity component can be combined and treated as one velocity component.

(2) The airflow is uniform.

(3) The air is at ambient temperature, so droplet evaporation can be neglected.

(4) The influence of different droplet velocities on the drop-size measurements made by the Malvern particle sizer is neglected.

The initial drop-size distribution can be expressed by $\bar{D}_0(SMD_0)$ and N_0 with the initial volume fraction $(dQ/dD)_0$ as

$$\left(\frac{dQ}{dD}\right)_o = \frac{N_o}{\bar{D}_o}\left(\frac{D}{\bar{D}_o}\right)^{N_o-1} \exp\left[-\left(\frac{D}{\bar{D}_o}\right)^{N_o}\right] \tag{3}$$

At a downstream distance x, the droplets of diameter D move from the origin and then distribute themselves on a circumference of radius $R(D)$ while the laser light beam of diameter d_j only meets some of these droplets:

$$\left(\frac{dQ}{dD}\right)_o \frac{2(\varphi_2 - \varphi_1)}{2\pi} \tag{4}$$

where

$$\varphi_1 = \arcsin \frac{y_o - \frac{1}{2} d_j}{R(D)} \tag{5}$$

$$\varphi_2 = \arcsin \frac{y_o + \frac{1}{2} d_j}{R(D)} \tag{6}$$

The definitions of φ_2 and φ_1 are shown in figure 5. When

$$y_o - \tfrac{1}{2} d_j \leq R(D) \leq y_o + \tfrac{1}{2} d_j$$

then

$$\varphi_2 = \frac{\pi}{2}$$

where y_o is the radial distance and d_j the diameter of the light beam.

The summation of the liquid fraction of the droplets of various diameters passing through the laser light beam is given by

$$\int_{D_{min}}^{D_{max}} \left(\frac{dQ}{dD}\right)_o \frac{\varphi_2 - \varphi_1}{\pi} dD \tag{7}$$

The minimum diameter D_{min} that the laser light beam can see is determined by

$$R(D_{min}) = y_o - \tfrac{1}{2} d_j$$

That is, at the downstream distance x, if $R(D) < y_o - 1/2\, d_j$, this droplet will not pass through the laser light beam. The relationship $R(D)$ can be determined by the droplet motion equation. The maximum diameter that may exist in the spray, can be approximated by

$$D_{max} = 3.5(SMD)$$

If we take the droplets within the laser light beam as a new spray (a sample), the liquid volume fraction of droplets of diameter D in this new spray (sample) is

$$\frac{dQ'}{dD} = \frac{\left(\frac{dQ}{dD}\right)_o \frac{\varphi_2 - \varphi_1}{\pi}}{\int_{D_{min}}^{D_{max}} \left(\frac{dQ}{dD}\right)_o \frac{\varphi_2 - \varphi_1}{\pi} dD} \tag{8}$$

Since this is actually the drop-size distribution of the sample (new spray) the laser light beam is to measure, we may obtain Q' as a function of D. Then, if we assume that the Rosin-Rammler (R-R) distribution can be used for data fitting the sample (new spray), we obtain new SMD' and N' for the sample. These values, SMD' and N', change with the distance y_o. If we delete the prime, we obtain the functional relationships SMD = f(y) and N = f(y).

DROPLET TRAJECTORY EQUATION

If we use a coordinate system which is moving with the airflow, then the droplet motion equation is

$$m \frac{dw}{dt} = -C_D \frac{\rho_a w^2}{2} s \tag{9}$$

where

m droplet mass, $(\pi/6)\rho_\ell D^3$

ρ_ℓ liquid density

w droplet relative velocity

C_D droplet drag coefficient, $C_D = 15/\sqrt{Re}$ for $Re = \rho_a DW/\mu_a$

ρ_a density of air

μ_a viscosity of air

Equation (9) can be rewritten as

$$\frac{d\left(\frac{W}{W_o}\right)}{dt} = -\frac{45}{4} \frac{(\rho_a \mu_a W_o)^{1/2}}{\rho_\ell} D^{-3/2} \left(\frac{W}{W_o}\right)^{3/2} \tag{10}$$

where W_o is the droplet initial relative velocity.

Integrating equation (10) yields

$$\frac{W}{W_o} = (Bt + 1)^{-2} \tag{11}$$

where

$$B = \frac{45}{8} \frac{(\rho_a \mu_a W_o)^{1/2}}{\rho_\ell} D^{-3/2} \tag{12}$$

We know that, at the downstream distance x, droplet velocity, air velocity, and the relative velocity of these two have the following relations:

$$V_x = V_a + (V_{xo} - V_a)\frac{W}{W_o}$$

and (13)

$$V_R = V_{Ro} \frac{W}{W_o}$$

where V_x and V_R are the axial and radial velocity components of the droplet, and V_{xo} and V_{Ro} are the initial values of these components. Thus, we obtain the droplet trajectory equations

$$\left.\begin{aligned} x &= V_a t + (V_{xo} - V_a) \int_o^t \frac{W}{W_o}\, dt \\ \text{and} \\ R &= V_{Ro} \int_o^t \frac{W}{W_o}\, dt \end{aligned}\right\} \tag{14}$$

From equation (11) we have

$$\int_o^t \frac{W}{W_o}\, dt = \frac{t}{Bt + 1} \tag{15}$$

From equations (14) and (15) we have the radial position (droplet size D) at downstream distance x:

$$R(D) = V_{Ro} \frac{1}{B + \frac{1}{t}} \tag{16}$$

Time t can be determined by

$$t = \frac{XB - V_{xo} + \left[(XB - V_{xo})^2 + 4V_a BX\right]^{1/2}}{2V_a B} \tag{17}$$

where B is determined by equation (12).

From equations (14) and (15), by substituting x and $R_{min} = R(D_{min}) = y_o - (1/2)\, d_j$, we obtain

$$D_{min} = \left[\frac{45}{8} \frac{(\rho_a \mu_a W_o)^{1/2}}{\rho_\ell} \frac{\frac{V_{xo} - V_a}{V_{Ro}} R_{min}^2 - XR_{min}}{V_{xo} R_{min} - xV_{Ro}}\right]^{2/3} \tag{18}$$

CALCULATION METHOD AND RESULTS

In order to calculate the variation of spray characteristics along the radial distance the following parameters must be known:

(1) Axial distance x
(2) Pressure drop across the nozzle ΔP_ℓ
(3) Fuel properties and physical properties of air
(4) Atomizer spray cone angle
(5) Initial spray characteristics $(SMD)_o$ and N_o

The calculation method used in this paper may be summarized as follows:

(1) Use the measured SMD and N values at $y = 0$ and the downstream distance x as the approximation of $(SMD)_o$ and N_o. We know that there is some difference between $(SMD)_o$ and $SMD_{y=0}$, N_o, and $N_{y=0}$ (ref. 2). So far these are the most reasonable approximate values that can be used.

(2) Calculate the initial droplet velocity $V_\ell = \mu(2\Delta p_\ell/\rho_\ell)^{1/2}$ where μ is the flow coefficient for the pressure drop. For the atomizer used in the present research, the spray angle is close to 90°; therefore,

$$\left.\begin{aligned} V_{xo} &= 0.566 \left(\frac{2\Delta p_\ell}{\rho_\ell}\right)^{1/2} \\ V_{Ro} &= 0.566 \left(\frac{2\Delta p_\ell}{\rho_\ell}\right)^{1/2} \end{aligned}\right\} \tag{19}$$

(3) Determine the D_{min} value for a different y_o value by equation (18). We assume $D_{max} = 3.5(SMD)$.

(4) Use the Simpson method to solve equation (8), with the $R(D)$ value calculated from equations (16) and (17).

(5) Determine the integration

$$Q' = \int_{D_{min}}^{D} \left(\frac{dQ'}{dD}\right) dD$$

From this, we are able to obtain a set of the data of Q' and D.

(6) Assume that Q' can be fitted by R-R distribution:

$$Q' = 1 - \exp\left[-\left(\frac{D}{\bar{D}'}\right)^{N'}\right]$$

By using the least-square method, we can obtain $\bar{D}$ and N'; then, SMD' and N' can be calculated. These SMD' and N' values are plotted against y in figures 6 to 13.

The results of the calculations for different airflow velocities and for the nozzle pressure drop are shown in figures 6 to 13. These are compared with the corresponding experimental data. It is obvious that the predictions are in excellent agreement with the experimental results.

CONCLUDING REMARKS

In the present study, droplet evaporation was neglected (discussed by J.S. Chin and J.Y. Zhu in the unpublished paper cited previously), and it is not difficult to take into consideration the effect of droplet evaporation.

After this model has been validated, it is relatively simple to predict the fuel distribution downstream of a pressure-swirl atomizer (ref. 6).

One interesting point that was noticed from the experiments and the analysis was that the larger droplets are always at the spray edge. Because the ignition spark plug is also always positioned close to the spray edge, the spark might meet the larger droplets, which would harm the ignition.

We measured the variation of spray characteristics along the radial distance was by laser light-scattering technology. And we found that the prediction based on the proposed spray model was in excellent agreement with the experimental data.

REFERENCES

1. J.S. Chin; R. Durrent; and A.H. Lefebvre: The Interdependence of Spray Characteristics and Evaporation History of Fuel Sprays. Transactions of ASME Journal of Engineering for Gas Turbine and Power. July, 1984.

2. J.S. Chin; D. Nickolaus; and A.H. Lefebvre: Influence of Downstream Distance on the Spray Characteristics of Pressure-Swirl Atomizers. ASME 85-GT-138, Transactions of the ASME, Journal of Engineering for Gas Turbine and Power, Jan., 1986.

3. L.G. Dodge; and C.A. Moses: Mechanisms of Smoke Reduction in the High Pressure Combustion of Emulsified Fuels. Vol. 1, Construction of Apparatus and Preliminary Experiments, Yearly Progress Report No. 1, Sept. 29, 1980 to Sept. 29, 1981.

4. M.H. Cao; J.S. Chin; et al.: Semi-Empirical Analysis of Liquid Fuel Distribution Downstream of a Plain Orifice Injector Under Cross-stream Air Flow. Transactions of the ASME, Journal of Engineering for Power, Oct., 1982.

5. J.S. Chin; X.F. Wang; W.M. Li; and A.H. Lefebvre: The Influence on Measured Spray Characteristics of Variations in the Radial and Angular Positions of the Sampling Laser Beam. Spring Technical Meeting Central States Section/The Combustion Institute, Paper CSS/CI 86-5C1, 1986.

6. J.S. Chin; and A.H. Lefebvre: Prediction of Liquid Fuel Distribution Downstream of a Swirl Atomizer in Flowing Air. Spring Technical Meeting, Central States Section/The Combustion Institute, Paper CSS/CI 83-20, 1983.

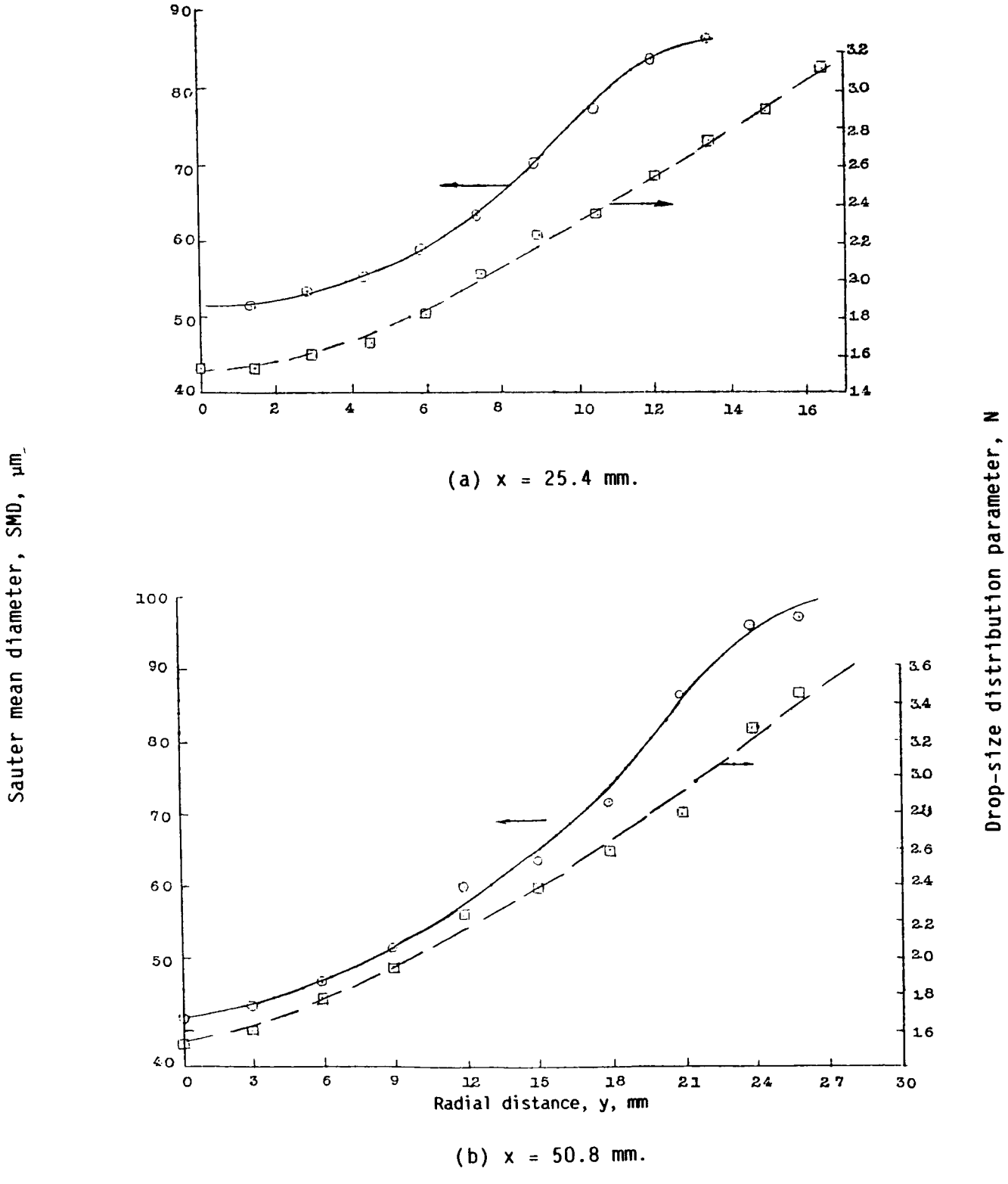

Figure 1. - Lee Dodge's measurement results (ref. 4). Atomizer pressure drop, ΔP, 100 lb/in.^{2}.

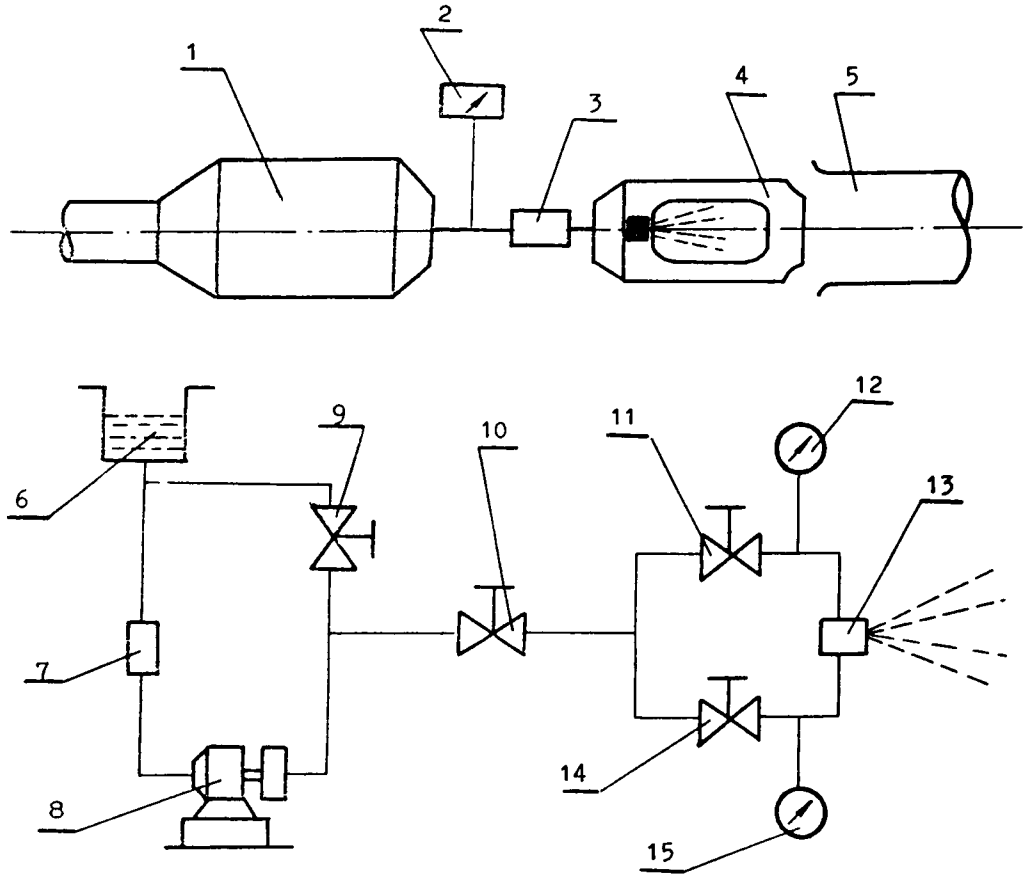

Figure 2. - Experimental system. Plenum chamber, 1; air temperature, 2; air flowmeter, 3; test section, 4; exhaust pipe, 5; fuel tank, 6; filter, 7; pump, 8; return valve, 9; valve, 10; pilot-fuel flow valve, 11; pressure gauge, 12; atomizer, 13; main-fuel flow valve, 14; pressure gauge, 15.

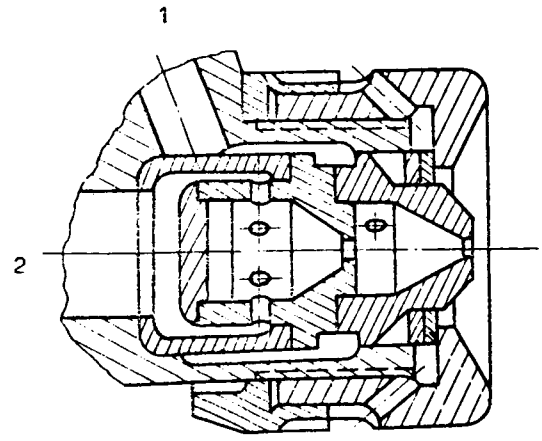

Figure 3. - Atomizer. Pilot-fuel flow, 1; main-fuel flow, 2.

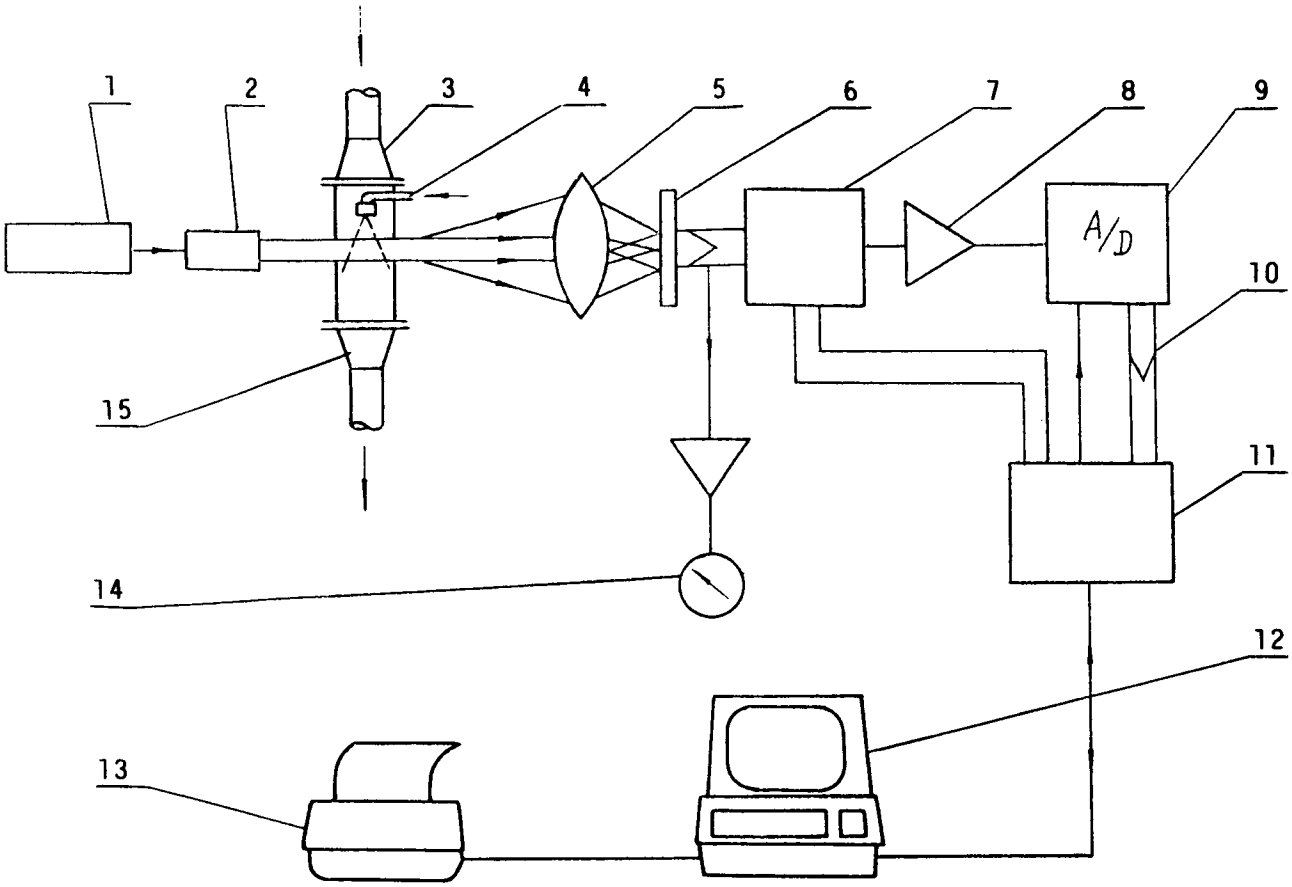

Figure 4. - Laser drop particle sizer. Laser, 1; beam expander, 2; test section, 3; fuel nozzle, 4; lens, 5; photo detector, 6; solid valve, 7; amplifier, 8; A/D converter, 9; data transfer, 10; interface, 11; computer, 12; printer, 13; micro tune, 14.

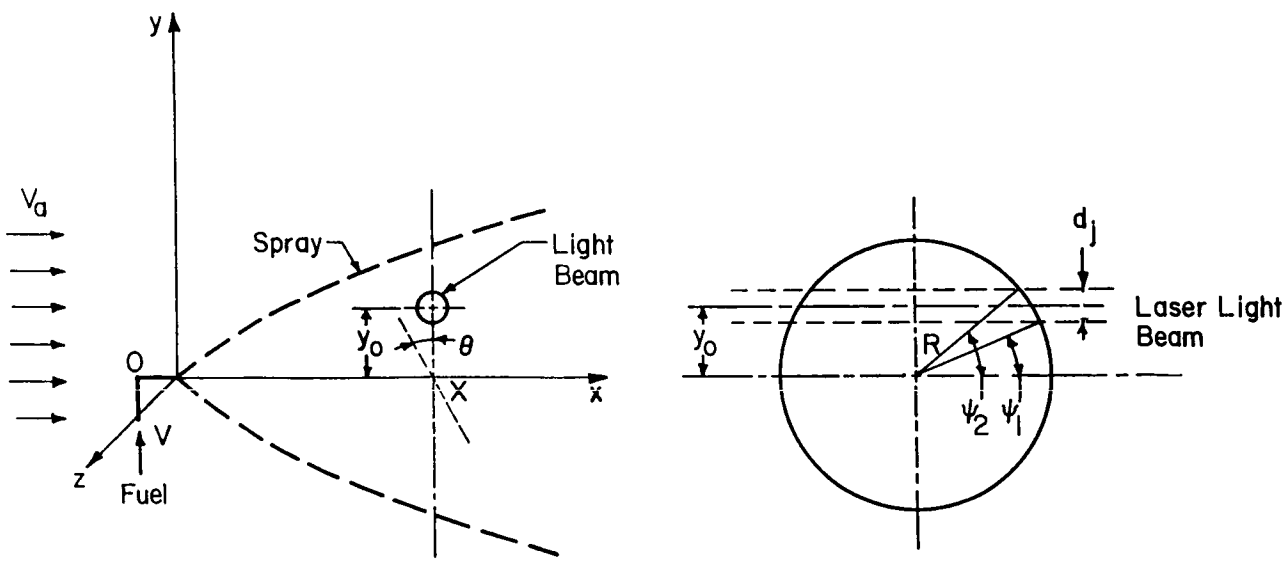

Figure 5. - Physical model.

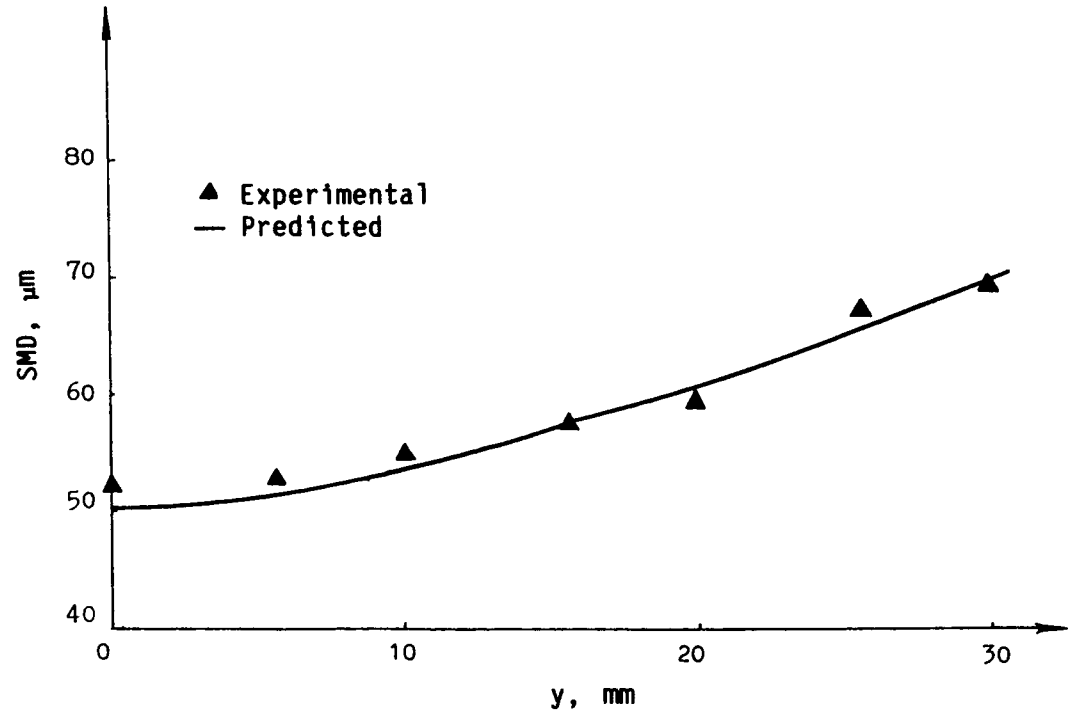

Figure 6. - Variation of Sauter mean diameter (SMD) along radial distance (y) for x = 70 mm, V_a = 9 m/sec, and ΔP = 12 kg/cm^2.

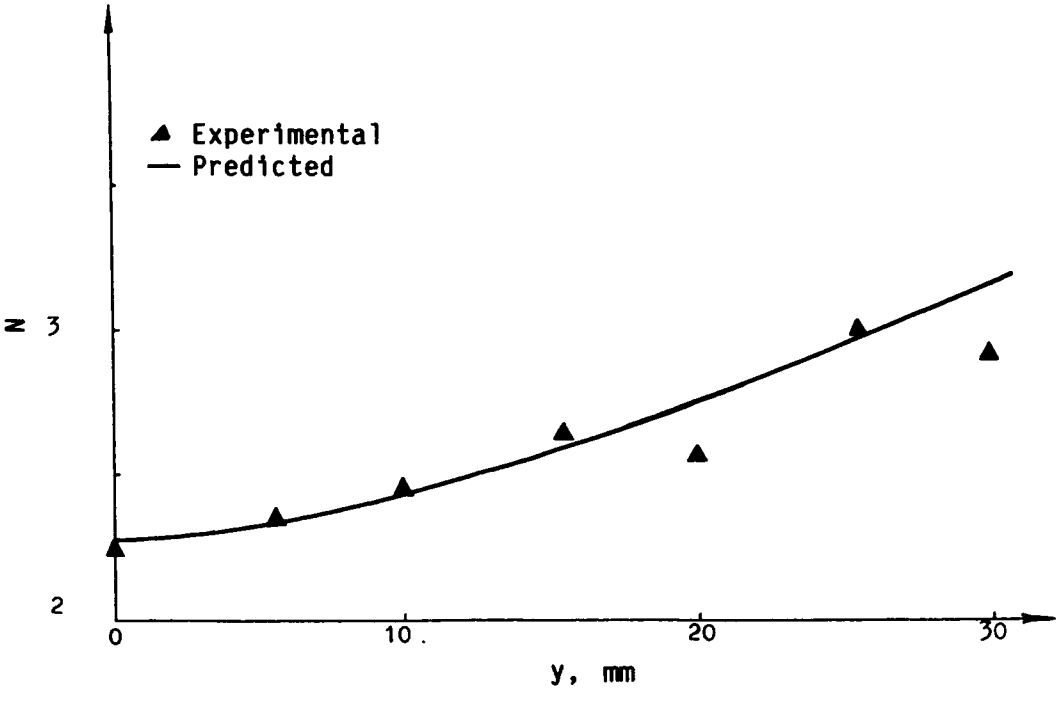

Figure 7. - Variation of drop-size distribution parameter (N) along radial distance (y) for x = 70 mm, V_a = 9 m/sec, and ΔP = 12 kg/cm^2.

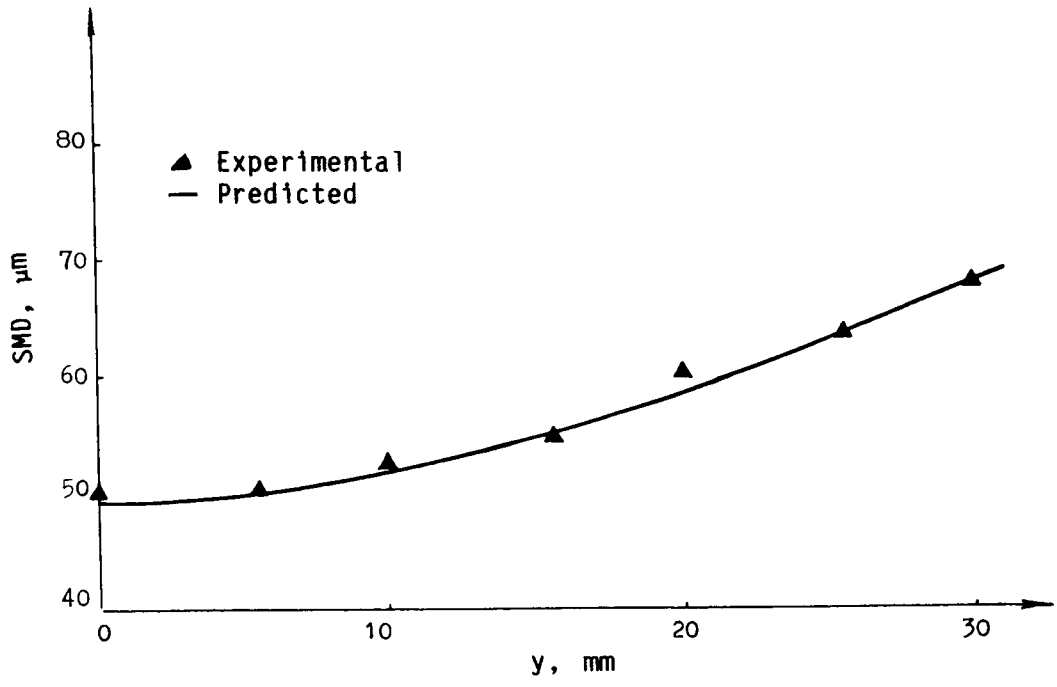

Figure 8. - Variation of Sauter mean diameter (SMD) along radial distance (y) for x = 70 mm, V_a = 6 m/sec, and ΔP = 12 kg/cm^2.

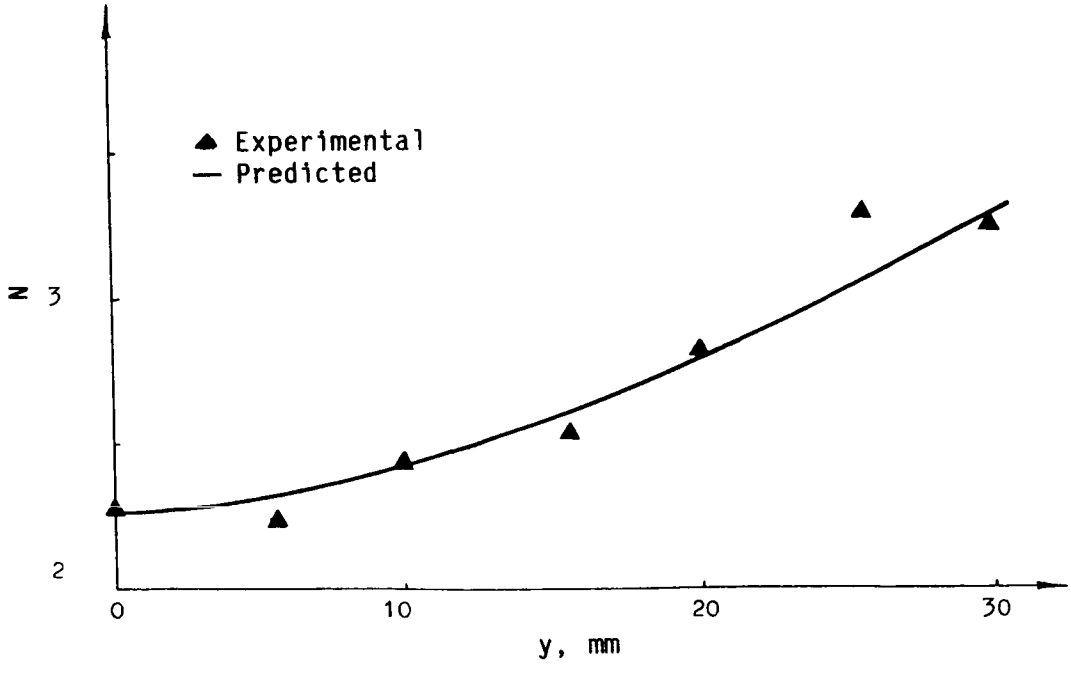

Figure 9. - Variation of drop-size distribution parameter (N) along radial distance (y) for x = 70 mm, V_a = 6 m/sec, and ΔP = 12 kg/cm^2.

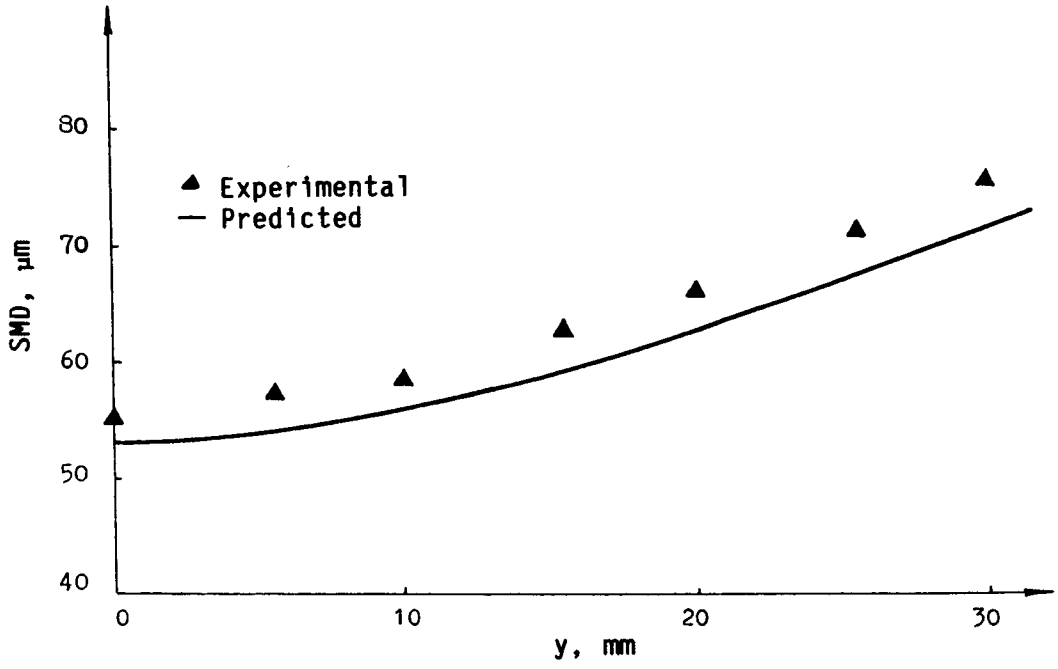

Figure 10. - Variation of Sauter mean diameter (SMD) along radial distance (y) for x = 70 mm, V_a = 6 m/sec, and ΔP = 8 kg/cm^2.

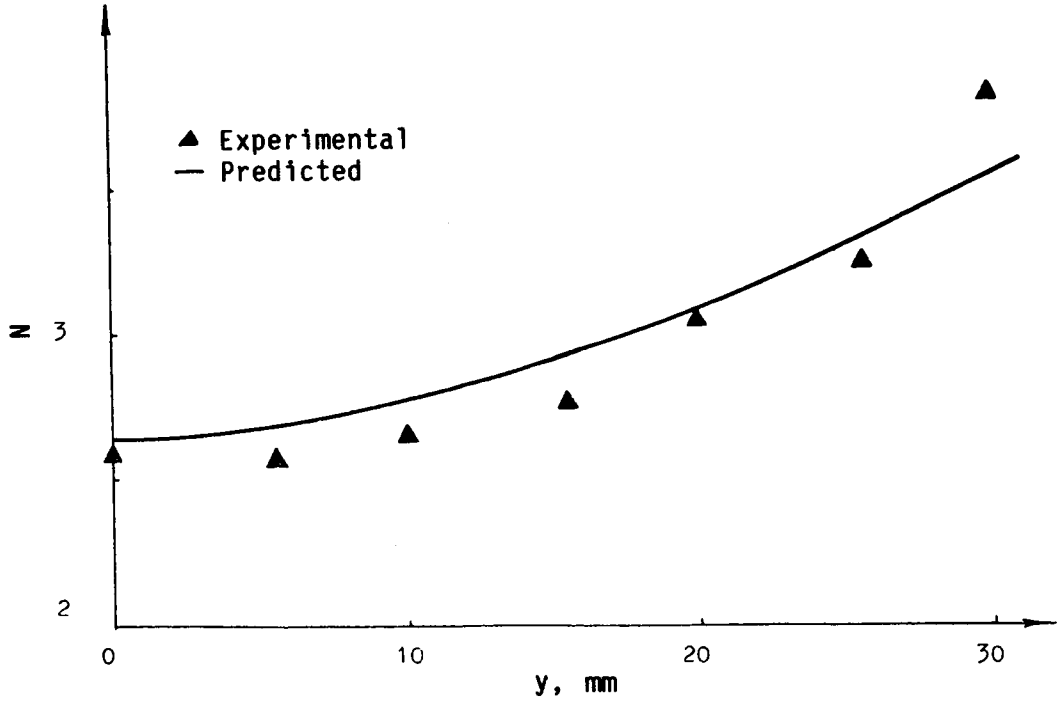

Figure 11. - Variation of drop-size distribution parameter (N) along radial distance (y) for x = 70 mm, V_a = 6 m/sec, and ΔP = 8 kg/cm^2.

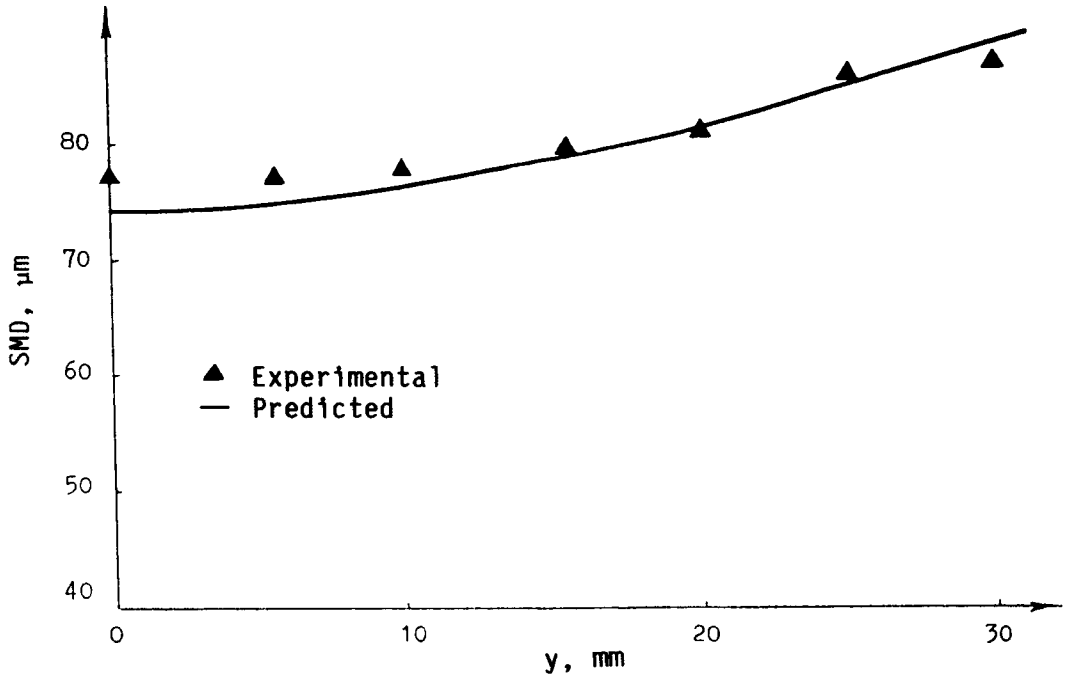

Figure 12. - Variation of Sauter mean diameter (SMD) along radial distance (y) for x = 70 mm, V_a = 6 m/sec, and ΔP = 4 kg/cm^2.

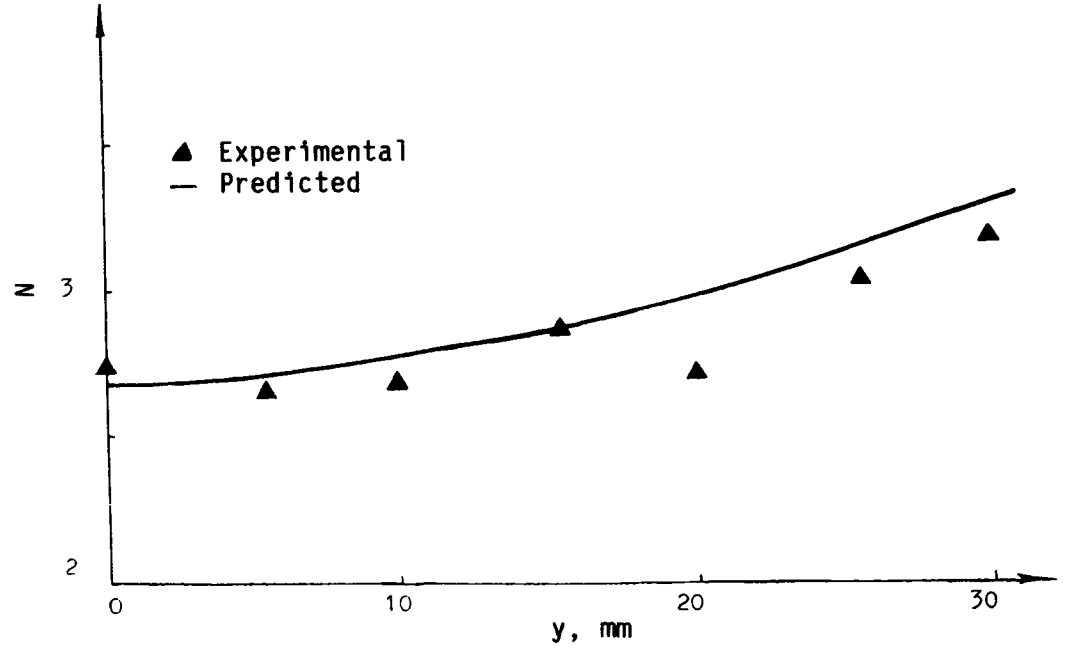

Figure 13. - Variation of drop-size distribution parameter (N) along radial distance (y) for x = 70 mm, V_a = 6 m/sec, and ΔP = 4 kg/cm^2.